J. Fluid Mech. (1987), *vol.* 176, *pp.* 253–264
Printed in Great Britain

Efflux from a slit in a vertical wall

By E. O. TUCK

Department of Applied Mathematics, University of Adelaide, GPO Box 498, Adelaide, SA 5001, Australia

(Received 12 March 1986)

A numerical solution is provided for flow of a stream of water falling under gravity after emerging from a simple slit orifice in a vertical wall. The classical free-streamline flow with contraction coefficient 0.611 applies in the absence of gravity, or as $F \to \infty$, where F is the Froude number based on the net volume flux and the slit width. We assume here that F is finite, but find that the flow exists only for $F \geqslant 0.496$, with initial backflow at the upper stream surface for $0.496 \leqslant F \leqslant 0.578$. The limiting flow at $F = 0.496$ has a stagnation point at the upper edge.

1. Introduction

The flow in figure 1 is very familiar (e.g. Batchelor 1967, p. 496). In two dimensions, it represents efflux of incompressible inviscid water from a slit in a plane wall, neglecting gravity. The flow upstream appears as if due to a sink at the origin, but becomes a jet, with constant-speed free surfaces that detach smoothly from the edges of the slit. Far downstream, the jet asymptotes to a straight uniform stream of width $\pi/(2+\pi) = 0.611$ times the slit width, this being the so-called 'contraction coefficient' of this particular orifice. The mathematical solution is well known and classical in two dimensions, and can be obtained in almost closed form via the hodograph transformation. Generalizations to more-complicated two- and three-dimensional orifices are easily obtained. Surface tension can also be included, but usually, and in the present work, is not.

So much for flows in the absence of gravity. If gravity is present, it may simply accelerate the flow if it acts exactly parallel to the downstream jet (e.g. if the wall is horizontal), and some studies (e.g. Conway 1967; Keady & Norbury 1975) have been made of this class of problem. The situation can be considerably more complicated if the wall is not horizontal, and to keep the problem as clear as possible, we treat here only the extreme case of a slit in a vertical wall lying in $x = 0$, with gravity in the $-y$-direction. Now the emerging jet is distorted downward by gravity, and eventually falls as an ever-thinner sheet in an asymptotically parabolic arc.

It is appropriate to define the Froude number

$$F = \frac{Q}{(gw^3)^{\frac{1}{2}}}, \tag{1.1}$$

where Q is the net volume efflux (per unit distance perpendicular to the plane of flow), g is the acceleration of gravity, and w the slit width. Then the classical flows in the absence of gravity are just the limit as $F \to \infty$, and can be approximated in very high-speed situations. There have been many large-F asymptotic studies, of which that by Geer & Keller (1979) is representative, in which one matches the gravityless classical orifice flow of figure 1 to a 'thin-jet' theory for the falling stream far from the orifice.

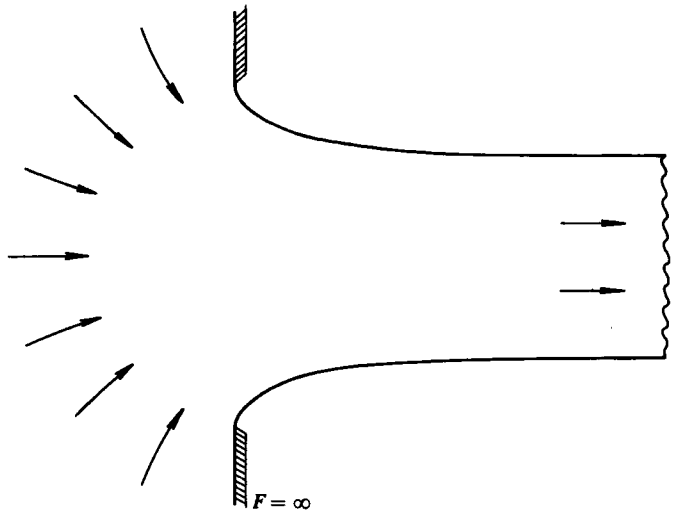

FIGURE 1. Classical free-streamline flow through an orifice, in the absence of gravity.

Our present aim is to treat instead the case when F is not large, and this appears to demand a full numerical approach. We first describe the problem in a suitable hodograph-type representation, in which the dependent variable is the angle $\theta(\xi)$ between the free surface and the x-axis, as a function of an independent variable ξ that lies within a finite interval $\xi_0 < \xi < \xi_N$, where $\xi = \xi_0 < 0$ is the top edge and $\xi = \xi_N > 0$ the bottom edge. The origin $\xi = 0$ represents the ultimate free-falling jet at $y = -\infty$.

In terms of $\theta(\xi)$, the problem becomes that of solving a nonlinear integral equation, namely that which results from setting the free-surface pressure equal to the constant atmospheric value, surface tension being neglected. This integral equation is solved by simple discretization, collocation, and iterative solution of algebraic equations. Considerable care is needed to account for singularities at $\xi = \xi_0, \xi_N$ and 0, and results are obtained to about 3-figure accuracy with discretizations involving 100 or less points.

For the particular problem of interest here, the computations show that solutions exist only for $F \geqslant F_0$, where $F_0 \approx 0.496$. Solutions for $F > F_0$ involve tangential detachment from the edges, so that, for example, $\theta = -\frac{1}{2}\pi$ at $\xi = \xi_0$. However, for $F_0 < F < F_1$, where $F_1 \approx 0.578$, the upper free streamline initially curves *back*, i.e. $\theta < -\frac{1}{2}\pi$ and $x < 0$ for a range of ξ close to ξ_0. Finally, at $F = F_0$, tangential detachment no longer occurs at the top edge, which becomes a stagnation point, with $\theta = -\frac{5}{6}\pi$. A separate numerical solution is provided for this limiting case, in which (in effect) the limiting Froude number F_0 itself is one of the unknowns of the problem.

In practice, if the flow is slowed down to $F < F_0$, where there exists no solution of the presently assumed type, some form of violent breakdown or ventilation may occur, in which surface tension and viscous effects, both neglected in the present theory, play important roles. Some simple observations of flows of this nature (carried out using a box-like nozzle on a garden hose) suggest that the critical Froude number for ventilation is indeed close to $F_0 = 0.5$. Proper experimental verification would be not too difficult.

There is a similarity between the present type of jet-like efflux flow and even

better-known efflux problems such as flow under sluice gates (see e.g. Budden & Norbury 1977) and over weirs (see e.g. Kandaswamy & Rouse 1957). The former configuration can be obtained by a simple modification of the present computer program, replacing the vertical lower half-wall by a horizontal full wall. Similarly, weir-like configurations can be obtained in the limit as the upper half-wall is taken away. Very recent work along these lines on both problems has been done by Vanden-Broeck (1986*b*), Vanden-Broeck & Keller (1986) and Goh (1986).

2. Mathematical formulation

We assume steady irrotational motion of an incompressible inviscid fluid in two dimensions. Thus the mathematical task can be described in terms of determination of suitable analytic functions of complex variables. The problem will be assumed to have already been rendered non-dimensional. In particular, we have set the net volume flux Q to unity and the water density (which plays no essential role here) also to unity. We make an arbitrary choice of lengthscale, and then determine the slit width w, as part of the solution of the problem. The Froude number F is thus also an output quantity, but is controlled by input values of gravity g.

If $\phi(x, y)$ is the velocity potential and $\psi(x, y)$ the stream function, we use complex variables $z = x + \mathrm{i}y$ and $f = \phi + \mathrm{i}\psi$. The flow takes place in the strip $-1 \leqslant \psi \leqslant 0$ in the f-plane, which we map to the lower-half ζ-plane by

$$\zeta = -\mathrm{e}^{-\pi f}. \tag{2.1}$$

The flow domains in the z-, f- and ζ-planes are sketched in figure 2. Note that the ultimate free-falling jet lies at $\phi \to +\infty$, which maps to the origin $\zeta = 0$ in the ζ-plane. The top and bottom edges of the slit are assumed to be at $\zeta = \xi_0$ and $\zeta = \xi_N$ respectively, where $\xi_0 < 0$ and $\xi_N > 0$ are (given) real parameters.

It is convenient to introduce a further complex variable, the logarithmic hodograph

$$\Omega = \log \frac{\mathrm{d}f}{\mathrm{d}z} \tag{2.2}$$

$$= \tau - \mathrm{i}\theta, \tag{2.3}$$

where $q = \mathrm{e}^{\tau}$ is the flow speed and θ its direction. In the first instance we seek the analytic function $\Omega = \Omega(\zeta)$.

By considering the imaginary part $-\theta$ of this variable, we can give an alternative real-variable interpretation of this task. That is, if $\zeta = \xi + \mathrm{i}\eta$, we seek the harmonic function $\theta = \theta(\xi, \eta)$ in the lower-half plane $\eta < 0$. The boundary conditions on $\eta = 0$ consist of specifications

$$\theta = -\tfrac{1}{2}\pi, \quad \eta = 0, \quad \xi < \xi_0 \tag{2.4}$$

and

$$\theta = +\tfrac{1}{2}\pi, \quad \eta = 0, \quad \xi > \xi_N \tag{2.5}$$

of the flow direction on the upper and lower portions of the wall, and constancy of the pressure, given by

$$p = -\tfrac{1}{2}q^2 - gy \tag{2.6}$$

on the free surface $\eta = 0, \xi_0 < \xi < \xi_N$. There is also a boundary condition at infinity in the ζ-plane, corresponding to the asymptote to a sink in the physical plane as $x \to -\infty$. This will be written in the form

$$\chi(\zeta) \to 0, \quad \text{as } |\zeta| \to \infty, \quad \eta < 0, \tag{2.7}$$

where

$$\chi = \Omega + \log \zeta + \mathrm{i}\tfrac{1}{2}\pi. \tag{2.8}$$

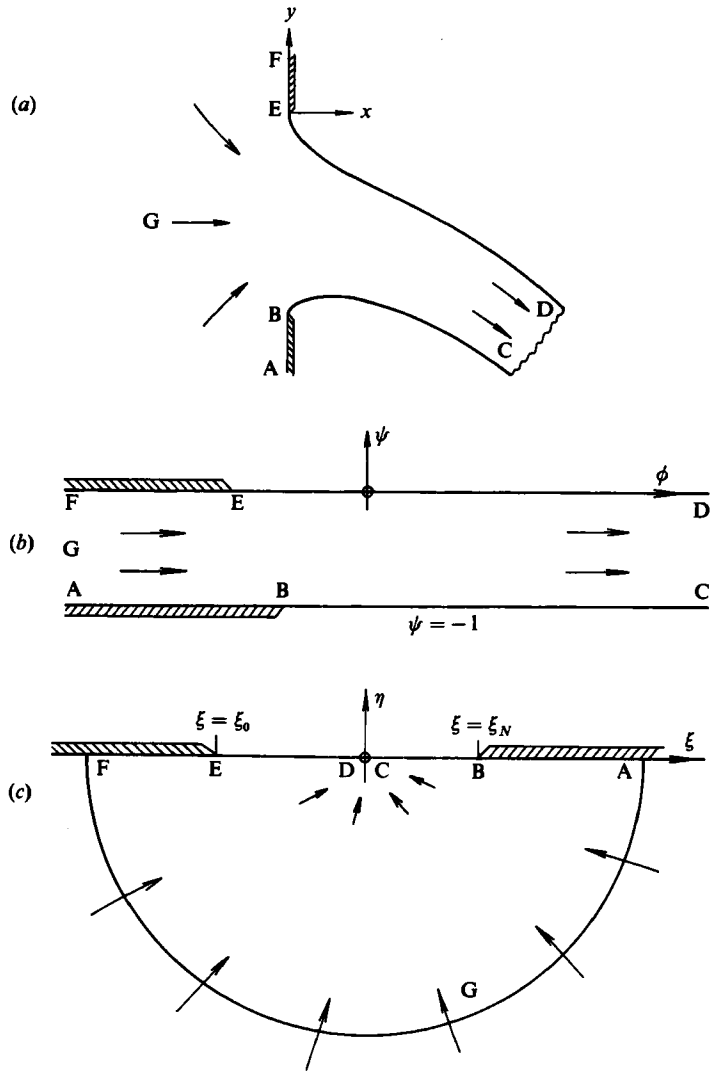

FIGURE 2. Sketch of flow in (*a*) the physical $z = x+\mathrm{i}y$ plane, and mappings to (*b*) $f = \phi+\mathrm{i}\psi$ and (*c*) $\zeta = \xi+\mathrm{i}\eta$ planes.

That is, $\tau \to -\log|\zeta|$ and $\theta \to \frac{1}{2}\pi + \arg\zeta$. Note that an arbitrary choice of scale has been made at this stage, since it would be possible to allow χ to tend to a real constant other than zero and still retain a sink-like behaviour.

The above boundary-value problem is nonlinear because of the free-surface condition (2.6), and indeed that condition requires considerable further discussion. In the first place, it involves two quantities q and y that do not have an immediately obvious relationship to the fundamental variable θ. To find the speed q, we need to find the harmonic conjugate τ to θ, and this can be done formally by use of Cauchy's theorem. It is convenient to use the variable $\chi(\zeta)$ defined by (2.8), since this vanishes at infinity in the lower-half ζ-plane. Thus, for real ζ, we have

$$\chi(\zeta) = -\frac{1}{\pi\mathrm{i}}\int_{-\infty}^{\infty}\frac{\chi(\xi)\,\mathrm{d}\xi}{\xi-\zeta}, \tag{2.9}$$

with a Cauchy principal-value interpretation. Substituting back for Ω from (2.8) and taking the real part yields the required relationship, namely

$$\tau(\zeta) = -\tfrac{1}{2}\log|\xi_0-\zeta| - \tfrac{1}{2}\log|\xi_N-\zeta| + \frac{1}{\pi}\int_{\xi_0}^{\xi_N}\frac{\theta(\xi)\,\mathrm{d}\xi}{\xi-\zeta}. \tag{2.10}$$

The boundary conditions (2.4) and (2.5) on the wall have been used to convert the infinite range of integration in (2.9) to the finite range (ξ_0, ξ_N) in (2.10). We have also taken the liberty of writing $\tau(\zeta)$ and $\theta(\zeta)$ for $\tau(\zeta,0)$ and $\theta(\xi,0)$ respectively, since from now on all computations will be confined to the boundary $\eta = 0$. Once $\theta = \theta(\xi)$ is known on the free surface $\xi_0 < \xi < \xi_N$, (2.10) formally provides τ on the free surface, and hence $q = \mathrm{e}^{\tau}$ for use in (2.6).

We still need the y-coordinate, for the hydrostatic part of the pressure. This is obtained by integrating (2.2), i.e.

$$z = \int \mathrm{e}^{-\Omega}\,\mathrm{d}f$$

or

$$z(\zeta) = \int_{\xi_0}^{\zeta} \mathrm{e}^{-\tau(\xi)+\mathrm{i}\theta(\xi)}\frac{\mathrm{d}\xi}{(-\pi\xi)}, \tag{2.11}$$

assuming without loss of generality that the top edge $\zeta = \xi_0$ is chosen as the origin in the z-plane. Thus

$$y(\zeta) = \int_{\xi_0}^{\zeta} \mathrm{e}^{-\tau(\xi)}\sin\theta(\xi)\frac{\mathrm{d}\xi}{(-\pi\xi)}. \tag{2.12}$$

A combination of (2.10) and (2.12) yields y, once $\theta(\xi)$ is known, and thus the pressure is fully determined.

The whole problem has thus reduced to a nonlinear integral equation, namely to determine $\theta = \theta(\xi), \xi_0 < \xi < \xi_N$, such that $p =$ constant, where p is given by (2.6), with q and y determined from $\theta(\xi)$ via (2.10) and (2.12). An important feature of this formulation is that this 'constant' value of p must itself be determined as part of the solution process.

Several points must be clarified before numerical solution of this integral equation is attemped. There are mild local singularities in $\theta(\xi)$ and $\tau(\xi)$ at $\xi = \xi_0, \xi_N$ and 0. The edge singularities at $\xi = \xi_0$ and $\xi = \xi_N$ are normally simple smooth-detachment conditions, with continuous slope but infinite curvature. For example, as $\zeta \to \xi_0$,

$$\theta \to \tfrac{1}{2}\pi + O(\zeta-\xi_0)^{\frac{1}{2}}, \tag{2.13}$$

and τ is bounded. However, in the special case (see later) where a stagnation point occurs at $\zeta = \xi_0, \theta(\xi_0+0) \neq \theta(\xi_0-0) = -\tfrac{1}{2}\pi$, and τ is unbounded, but the singularity is still only logarithmic, so Cauchy's theorem remains valid.

The singularity at $\xi = 0$ models the ultimate free-falling jet, and has a complicated structure, but is very mild as far as $\Omega(\xi)$ itself is concerned. Thus, as $\xi \to 0$, we have $\theta \to -\tfrac{1}{2}\pi$, while $\tau \to +\infty$ like '$\log\log|\xi|$'. However, a major difficulty occurs with (2.12), in which the 'stretching' factor '$-\pi\xi$' in the denominator makes it essentially impossible to integrate through $\xi = 0$. Instead, we use (2.12) only for $\zeta < 0$, and write for $\zeta > 0$

$$y(\zeta) = y(\xi_N) + \int_{\xi_N}^{\zeta} \mathrm{e}^{-\tau(\xi)}\sin\theta(\xi)\frac{\mathrm{d}\xi}{(-\pi\xi)}. \tag{2.14}$$

This has 'solved' the problem at the expense of introducing the so-far unknown y-coordinate $y(\xi_N) = -w$ of the lower edge. The latter is itself determinable from a knowledge of $\theta(\xi)$ by integrating upstream.

To do this, we first fit an extended representation

$$\tau = -\log|\zeta| + A\zeta^{-1} + B\zeta^{-2} + O(\zeta^{-3}) \tag{2.15}$$

of the asymptotic sink-like behaviour far upstream (cf. (2.7), (2.8)) to computations from (2.10) for large negative ζ, i.e. far up the upper wall, so determining the real constants A and B. An equivalent representation of the actual physical-plane variable $z = x + iy$ far upstream is

$$\pi i z = \zeta - A\log\zeta + \pi i + C + (B - \tfrac{1}{2}A^2)\zeta^{-1} + O(\zeta^{-2}), \tag{2.16}$$

where C is another real constant, determined this time by fitting to computations from (2.12). But (2.16) applies not only for real ζ as $\zeta \to -\infty$, but also as $|\zeta| \to \infty$ at any non-positive angle, and in particular applies for large real positive ζ, i.e. far down the lower wall. Hence it must also fit to computations from (2.14) for large positive ζ, and this immediately determines $y(\xi_N)$.

Although we have concentrated on the y-coordinate, since that plays an immediate role in determining the pressure, it is convenient and computationally efficient to determine simultaneously the x-coordinate, and in particular $x(\xi_N)$. Since there is no reason in general to expect that the latter quantity will be zero (indeed, it is clear from (2.16) that $x(\xi_N) = -A$), we are not really solving for flow through a slit in a plane wall, but rather for a more general geometrical configuration, involving two plane parallel walls. The special case $x(\xi_N) = 0$ when the offset between these two walls is zero, is available to us by suitable choice of the input parameters ξ_0 and ξ_N.

3. Numerical method

The nonlinear integral equation $p =$ constant converts to a set of N nonlinear algebraic equations in N unknowns, if we approximate integration by summation in a suitable manner. First we must select a set of interval end-points $\xi = \xi_j, j = 1, 2, \ldots, N-1$, where $\xi_0 < \xi_1 < \ldots < \xi_{N-1} < \xi_N$, and then we let $\theta_j = \theta(\xi_j), j = 1, 2, \ldots, N-1$, be $N-1$ of these unknowns, the Nth being the value of the pressure p on the free surface. Now, in order to evaluate the Cauchy principal-value singular integral in (2.10), we approximate $\theta(\xi)$ as varying linearly on the interval (ξ_{j-1}, ξ_j), and evaluate the integral over each such interval exactly. This can be done at any value of ζ, and we choose to do it on a separate grid $\zeta = \zeta_i$, where $\xi_{i-1} < \zeta_i < \xi_i$, with ζ_i close to the mid-point of the ith interval. Thus now $\tau(\zeta_i)$ can be computed as a linear sum over values of θ_j.

Similarly, the integrals (2.12) and (2.14) determining the y-coordinate of the free surface can be evaluated by a numerical quadrature on either of the above grids. Since these are non-singular integrals, the ordinary trapezoidal rule is satisfactory, and was applied on the ζ-grid. For this purpose, it was also necessary to interpolate linearly the θ-values from the ξ-grid. For $\zeta > 0$, (2.14) needs a value of $y(\xi_N)$, and this is obtained by the upstream integration described above.

In fact, the numerical determination of $y(\xi_N)$ consumes a significant proportion of the total computer time. The integral (2.10) for τ is evaluated for large $|\zeta|$, and results from it are then used in (2.12) and (2.14), also for large $|\zeta|$. The latter integrations in $\xi < \xi_0$ and $\xi > \xi_N$ were done by Simpson's rule on an equally spaced grid with an interval of the order of 0.1 times $(\xi_N - \xi_0)$, adequate for five-figure accuracy. In order to maintain the same accuracy in fitting to the far-field representations (2.15) and (2.16), we need to integrate as far as the order of 100 times $(\xi_N - \xi_0)$.

Once all of the above numerical integrations are performed, we have in effect a function subroutine that determines N functions

$$P_i(\theta_j) = p(\theta_j) - \theta_N \tag{3.1}$$

of the N unknowns $\theta_1, \theta_2, \ldots, \theta_{N-1}$ and θ_N, remembering that θ_N is the to-be-determined constant value of the free-surface pressure. Our final numerical task is to solve the equations $P_i = 0$, for which there are many good methods. Some success was achieved with the packaged (IMSL) routine 'ZSPOW', but a 'custom-built' approximate Newton iteration procedure proved as satisfactory and a little faster. At any fixed value of N, it is only necessary to solve these equations to an accuracy a little better than that required in the final answers, and we demand the same five-figure accuracy here as in the numerical integrations already performed to determine $y(\xi_N)$.

The real accuracy question then relates to the error in the fundamental discretization, i.e. to the extent and rate of convergence as $N \to \infty$. This is in turn affected by the choice of the grids $\{\xi_j\}$ and $\{\zeta_i\}$, a matter that has been so far left open. Any reasonable grid allows convergence of some sort, but only if the grid is suitably non-uniform, with points concentrated (correctly) near the singularities at $\xi = \xi_0, \xi_N$, and 0, can a rapid rate of convergence be achieved.

For the most part, we use the choice (cf. Goh & Tuck 1985)

$$\xi_j = \xi_0 \mathrm{e}^{-j^2\alpha}, \quad j = 1, 2, \ldots, M-1, \tag{3.2}$$

where α is a positive constant assigned below, and $M-1 < N$ is the number of interval end points on the upper free surface, $N-M$ being on the lower free surface. (We generally use M values about 60% of N, since the upper free surface is more 'busy' than the lower.) The Mth end point $\xi_M = 0$ is placed exactly at the origin in the ζ-plane, i.e. at downstream infinity. For $j > M$, we replace j in (3.2) by $N-j$, ξ_0 by ξ_N, and use a different constant α. The equivalent 'quasi-mid-point' grid $\{\zeta_i\}$ is obtained by replacing j by $i-\frac{1}{2}$ in the above. The constants α are determined by demanding that the two quasi-mid-points that are closest to the origin $\zeta = 0$, namely $\zeta = \zeta_M$ and $\zeta = \zeta_{M+1}$, be a prescribed (equal) small distance ϵ from it. For example, to use in (3.2) for $j < M$, we set

$$\alpha = -\frac{1}{(M-\frac{1}{2})^2} \log\left(-\frac{\epsilon}{\xi_0}\right). \tag{3.3}$$

Then the points $\zeta_M = -\epsilon$ and $\zeta_{M+1} = +\epsilon$ map in the physical plane to the furthest points downstream, on the upper and lower free surfaces respectively, and the small parameter ϵ controls the effective downstream truncation point.

The grid (3.2) accounts for a square-root singularity at $\xi = \xi_0$ and $\xi = \xi_N$, and a logarithmic singularity at $\xi = 0$. In fact, the exponential character of the grid near $\xi = 0$ models a uniformly spaced grid in terms of the original potential ϕ. We use values of ϵ of the order of 10^{-5}, so that ϕ is only as large as the order of 5 at the downstream truncation point but this is enough for negligible (to five figures) upstream influence of that truncation. This is in any case what one should expect, since such an influence arises from a contribution from an interval of length of the order of 10^{-5} to the integral (2.10). Because ϵ is so small, it is not too critical to build the asymptotic form of the far-downstream jet into the model. In fact, we allow the program to determine a value of $\theta_M = \theta(\xi_M)$ for itself, even though we know that $\theta(0) = -\frac{1}{2}\pi$. The output value of θ_M can be thought of as the mean flow direction across the jet at the downstream truncation section, and it is generally quite a bit less negative than $-\frac{1}{2}\pi$, as the results to follow show.

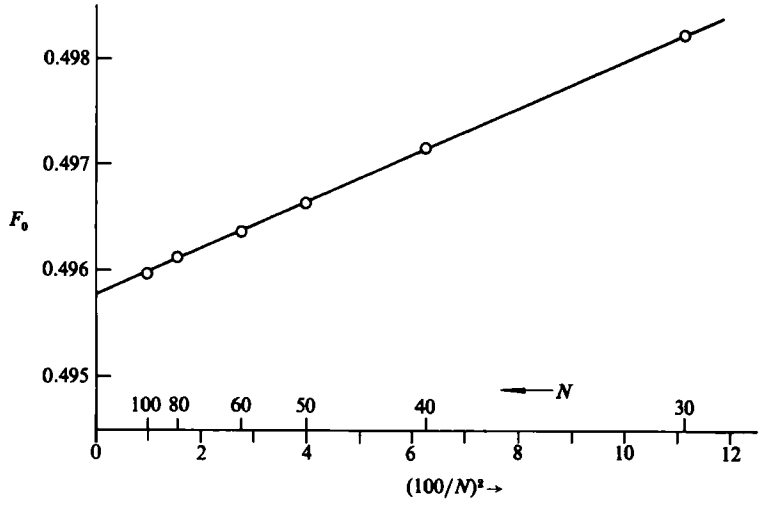

FIGURE 3. Output critical (minimum) Froude number F_0 for flow with stagnation point, as a function of the number N of points into which the free surface is discretized.

The above grid is used for cases where tangential detachment occurs from the wall edges, which is most of the time. In practice, given a specification of the locations $\xi = \xi_0$ and $\xi = \xi_N$ of these edges, we input the gravity parameter g, small at first, so that the classical solution yields a good starting guess for the unknowns θ_j, then slowly increase g using the converged solutions at lower g as a new starting guess. Once converged results are obtained at any g, the slit width $w = -y(\xi_N)$ is available to give the Froude number F defined by (1.1) (with $Q = 1$), and the output (x, y)-values along the free surface can also be re-scaled by dividing by w.

The process of increasing g eventually fails at some g to yield convergence of the algorithm for solution of the nonlinear algebraic equations. It is believed that no solution then exists to these equations, and by implication, to the original continuum problem, at this and all higher values of g.

This breakdown is signalled by a rapid decrease of $\tau(\zeta_1)$ toward $-\infty$, indicating a trend toward a stagnation point at $\xi = \xi_0$ at which tangential detachment no longer occurs. A separate program was written to solve the problem at the critical value of g, in which such a stagnation point was assumed to exist. In this program, we can no longer assign the last unknown θ_N to be the free-surface pressure, since the latter quantity is now necessarily zero. Instead, and with no extra difficulty, we use as our last unknown $\theta_N = g$ itself, so determining the critical value of g directly, and hence (after suitably re-scaling) the critical Froude number F_0.

Although this special stagnation-point program worked as described above with no further changes, in order to achieve the same accuracy as the non-stagnation program, some adjustments in the grid and the numerical integration procedures were needed. It is not hard to see (e.g. Grant 1973; Goh 1986; Vanden-Broeck 1986*a*) that when there is such a free-surface stagnation point, the velocity $q = e^{\tau}$ behaves like $(\xi - \xi_0)^{\frac{1}{3}}$ near $\xi = \xi_0$, and hence a cubic rather than a quadratic grid is needed. This is easily accomplished by replacing the power 2 by 3 in (3.2) and (3.3). At the same time, the integration in (2.12) needs to recognize the fact that its integrand has an inverse cube-root singularity, and a simple modification of the trapezoidal rule was implemented for about the first $M/4$ intervals.

The net effect of all of the above-described numerical approximations was to achieve an error decay like N^{-2} for both types of program. This is confirmed by

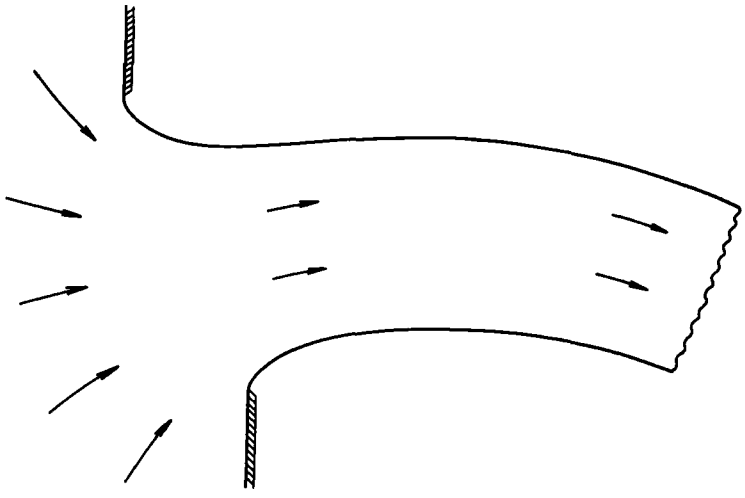

FIGURE 4. A typical computed flow from an x-wise offset orifice.

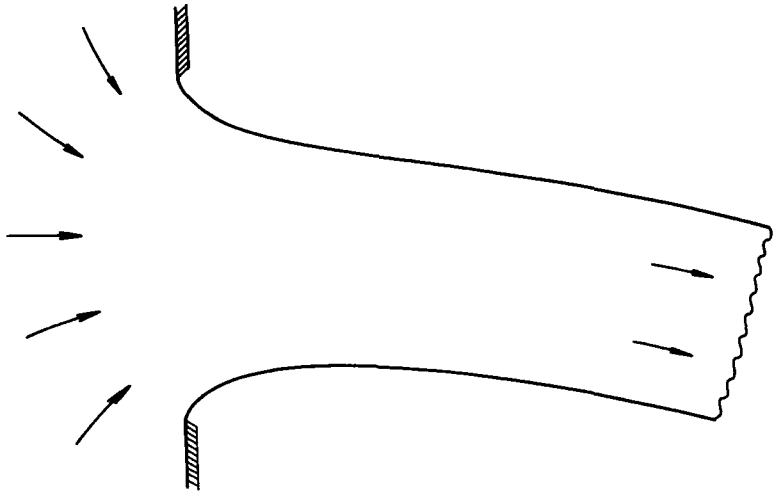

FIGURE 5. Efflux at a relatively high Froude number $F = 1.150$.

figure 3, which shows that the final output F_0 from the stagnation-point program is a linear function of N^{-2}. Extrapolation to $N^{-2} = 0$ gives $F_0 \approx 0.4958$. Three-figure accuracy is available even without extrapolation, from about $N = 60$ up. It is worth commenting that the somewhat similar numerical method used by Goh & Tuck (1985) achieved only N^{-1} convergence, mainly because a tangential differentiation of the Bernoulli free-surface conditions was used. The price paid for a better convergence rate in the present work is the computer time needed to evaluate $y(\xi_N)$, and this appears to be a price worth paying.

4. Results

As noted in §2, for a general input free-surface segment (ξ_0, ξ_N), the horizontal offset $x(\xi_N)$ between top and bottom walls cannot be expected to be zero. Without loss of generality, we can always take $\xi_N = 1.0$, and then the flows of interest have $\xi_0 < -1.0$. In such cases, if g is small, $x(\xi_N) > 0$ and the offset orifice tends to throw

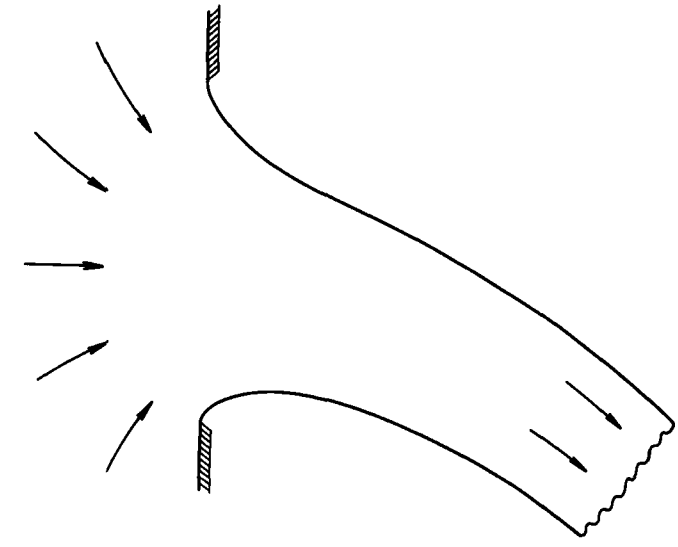

FIGURE 6. Efflux at a moderate Froude number $F = 0.728$.

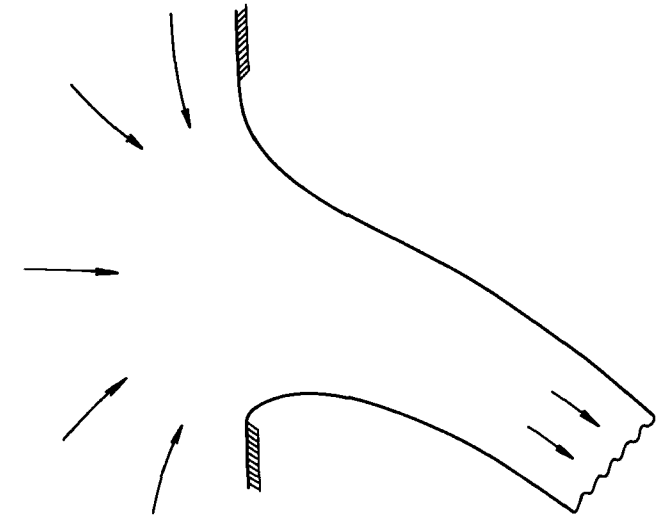

FIGURE 7. Efflux at $F = 0.578$, where the curvature vanishes at upper detachment.

the emerging jet upwards. At $g = 0$, this upward motion necessarily continues for ever, but for small $g > 0$ the jet eventually starts to fall. For example, figure 4 shows results from $(\xi_0, \xi_N) = (-2.6, 1.0)$ at $g = 0.4$, for which $(x(\xi_N), y(\xi_N)) = (0.6149, 1.3252)$.

If we now increase g, the offset $x(\xi_N)$ will decrease, and at some value of g (determined by trial and error), will pass through zero, so yielding solutions for the problem first posed, namely flow through an orifice in a plane vertical wall. Figures 5–8 show flows of this nature at various Froude numbers. For example, that in figure 8 is, like that of figure 4, for $(\xi_0, \xi_N) = (-2.6, 1.0)$, but for a much higher effective gravity, namely $g = 1.901$, sufficient to eliminate any tendency of the jet to rise. Each of the flows in figures 5–8 corresponds to a different value of ξ_0. As ξ_0

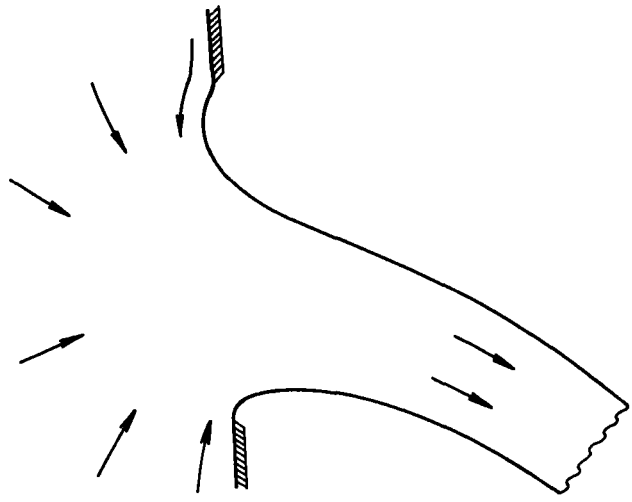

FIGURE 8. Efflux at $F = 0.508$, with backflow after initial tangential upper detachment.

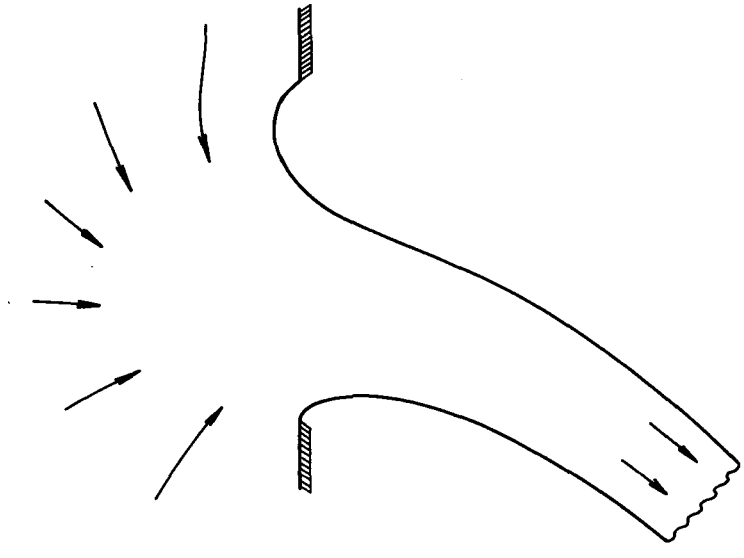

FIGURE 9. Efflux at $F = F_0 = 0.496$, with a stagnation point at the upper detachment, the free streamline there making 120° with the wall.

decreases, it becomes more and more difficult to achieve a zero offset $x(\xi_N)$ at g-values below that at which a stagnation point develops, and in fact that shown in figure 8 is the nearest to stagnation that was attempted using the non-stagnation program.

The reason for the difficulty as stagnation conditions are approached is clearly that large curvatures are induced, the upper free surface being forced to detach tangentially, i.e. vertically downward, but then to curve backwards quickly before reversing curvature to flow down and out. Backward flow occurs for $F < 0.578$, and the flow of figure 7 marks the borderline between flows that do and do not have an initial backward motion near the upper detachment point.

The downstream truncation point shown by the termination of the above figures on the right is that corresponding to $\epsilon = 10^{-5}$. Reduction of this parameter below 10^{-5} serves mainly the purpose of displaying more of the downstream jet, without significantly affecting the accuracy of the computation, and is hardly worthwhile. Note that even though our computations extend to within $|\zeta| = 10^{-5}$ of the point $\zeta = 0$ that maps downstream infinity, the jet is still very far from being well approximated by a thin parabolic arc at the truncation section.

Finally, figure 9 shows the limiting flow at $F = F_0 \approx 0.496$, with a stagnation point at $\xi = \xi_0$, and detachment at $\theta = -\frac{5}{6}\pi$.

REFERENCES

Batchelor, G. K. 1967 *An Introduction to Fluid Dynamics*, Cambridge University Press.

Budden, P. J. & Norbury, J. 1977 Sluice-grate problems with gravity. *Math. Proc. Camb. Phil. Soc.* **81**, 157–175.

Conway, W. E. 1967 The two-dimensional vertical jet under gravity. *J. Math. Anal. Appl.* **19**, 282–290.

Geer, J. & Keller, J. B. 1979 Slender streams. *J. Fluid Mech.* **93**, 97–115.

Goh, M. K. 1986 Numerical solution of quadratically nonlinear boundary-value problems using integral equation techniques, with application to jets and nozzle flows. Ph.D. thesis, University of Adelaide.

Goh, M. K. & Tuck, E. O. 1985 Thick waterfalls from horizontal slots. *J. Engng Maths* **19**, 341–349.

Grant, M. A. 1973 The singularity at the crest of a finite-amplitude progressive Stokes wave. *J. Fluid Mech.* **59**, 257–262.

Kandaswamy, P. K. & Rouse, H. 1957 Characteristics of flow over terminal weirs and sills. *J. Hydraulics Div. ASCE* **4**, 1–13.

Keady, G. & Norbury, J. 1975 The jet from a horizontal slot under gravity. *Proc. R. Soc. Lond.* A **344**, 471–487.

Vanden-Broeck, J.-M. 1986*a* Pointed bubbles rising in a two-dimensional tube. *Phys. Fluids* **29**, 1343–1344.

Vanden-Broeck, J.-M. 1986*b* Flow under a gate. *Phys. Fluids* **29**, 3148–3151.

Vanden-Broeck, J.-M. & Keller, J. B. 1986 Pouring flows. *Phys. Fluids* **29**, 3958–3961.